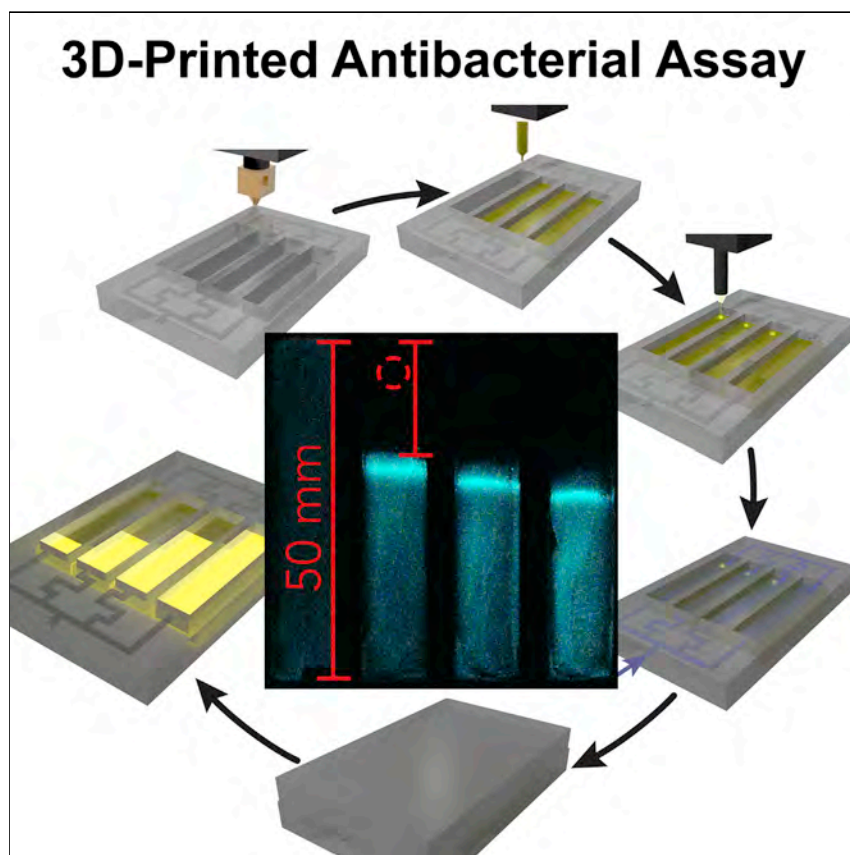


Article

A Portable 3D Printer System for the Diagnosis and Treatment of Multidrug-Resistant Bacteria



Cronin and colleagues present the use of 3D printing to manufacture and formulate antibiotics and test them in place as an alternative approach to tackling the challenge of multidrug-resistant bacteria. The robotic setup produces millifluidic devices that are filled automatically with growth medium, and antibiotics are formulated with the help of ink-jet technology. The tests are incubated in place with the heat of the 3D printer.

Stefan Glatzel, Mohammed Hezwani, Philip J. Kitson, Piotr S. Gromski, Sophie Schürer, Leroy Cronin

lee.cronin@glasgow.ac.uk

HIGHLIGHTS

Using 3D printing to manufacture antibiotic testing devices

Using ink-jet technology to formulate and test antibiotics

Parallelization and automation of antibiotic testing

Stand-alone system for the manufacture of tests and subsequent incubation in place



Glatzel et al., Chem 1, 494–504

September 8, 2016 © 2016 The Authors.

Published by Elsevier Inc.

<http://dx.doi.org/10.1016/j.chempr.2016.08.008>

Article

A Portable 3D Printer System for the Diagnosis and Treatment of Multidrug-Resistant Bacteria

Stefan Glatzel,¹ Mohammed Hezwani,¹ Philip J. Kitson,¹ Piotr S. Gromski,¹ Sophie Schürer,¹ and Leroy Cronin^{1,2,*}

SUMMARY

Multidrug-resistant bacteria are a major threat to human health, but broad-spectrum antibiotics are losing efficacy. There is a need to screen a given drug against a bacterial infection outside of the laboratory. To address this need, we have designed and built an inexpensive and easy-to-use 3D-printer-based system that allows easily readable quantitative tests for the performance of antibacterial drugs. The platform creates a sterile diagnostic device by using 3D printing, and the device is filled automatically with growth medium, and then antibiotics are sprayed onto the medium by ink-jet technology. The sample for testing can be introduced via a fluid port, and the printer hot bed is used to incubate the device, allowing operation in the field. Combining advantages from various established tests of antibacterial performance, this allows the comparison of a specific antibiotics and bacteria. Also, this system can create and test several antibiotic formulations for therapeutic use, and we demonstrate this potential by investigating a mixture of pathogens that are only killed by a mixture of drugs.

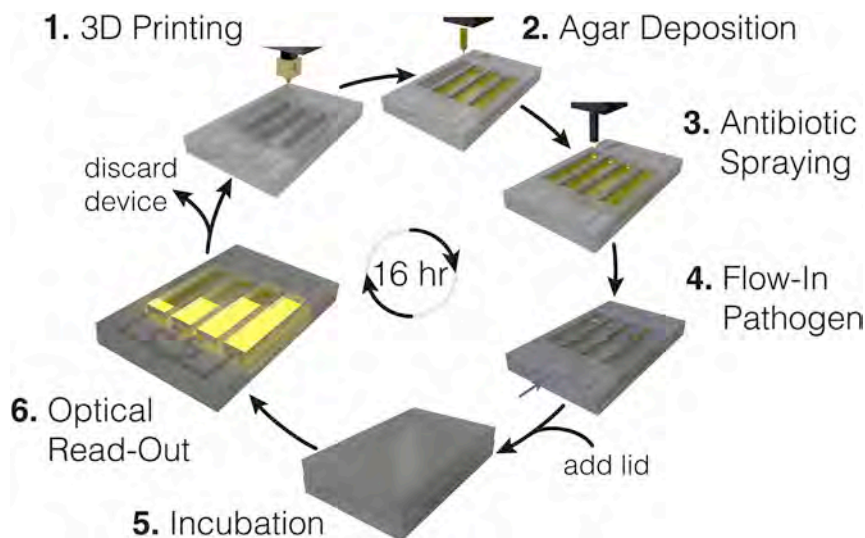
INTRODUCTION

The overuse of broad-spectrum antibiotics has created a tremendous problem for the future of human health. This is because bacteria are gradually becoming resistant to a wide range of antibiotics, resulting in the emergence of multidrug-resistant microorganisms or “super bugs.”¹ Often, such super bugs have become resistant to all but the most toxic drugs, and even these will soon be rendered useless.² Thus, previously trivial infections will increasingly prove to have potentially lethal consequences, including a dramatic impact on all aspects of health care because even routine hospital procedures could be fatal. Presently, several strategies are being used to counter what is being described as the single biggest threat to human health in the 21st century. These include the development of new drugs, which can take decades, or the selective use of antibiotics rather than broad spectrum antibiotics to prevent the development of drug-resistant bacteria. The critical problem is that selective drug use requires efficient, cheap, and fast diagnostic tests to identify the most effective drug, or combination of drugs, to ensure optimal treatment.^{3,4} Current antibiotic testing takes time and requires a highly equipped laboratory and trained personnel to first extract, culture, and subsequently isolate pathogens, which can then be tested against several antibiotics. Wide testing therefore creates enormous bottlenecks within hospitals and increased costs for patient care, as well as potentially worse outcomes as a result of the delayed tests, which can have extreme effects on a patient’s quality of life.

To explore this issue, we hypothesized that it should be possible to develop an inexpensive and autonomous system that produces a monolithic 3D-printed⁵ diagnostic

The Bigger Picture

The overuse of broad-spectrum antibiotics has created a tremendous human health problem because bacteria are becoming resistant to a wide range of antibiotics, resulting in the emergence of multidrug-resistant “super bugs” requiring selective drug treatment. The problem is that selective drug use requires highly equipped laboratories to determine the best drugs to be used. In this article, we present a solution to this problem whereby we were able to develop an inexpensive and autonomous system that produces 3D-printed diagnostic devices and is also capable of incubating them if needed, thereby leading to an autonomous and integrated system that can determine drug effectiveness against bacterial infection. This system is fully automated and combines three elements—plastic printing, gel deposition, and drug (such as antibiotics) spraying—by means of an ink-jet array to yield fully independent diagnostic units that can be used in hospitals, in the offices of general practitioners, at home, or in the field.



Scheme 1. Diagram Showing How Our Autonomous System Produces the Device

Steps are as follows: (1) 3D printing (FDM) of the device (~3 hr); (2) deposition of agar into all lanes (~2 min); (3) ink jetting of the antibiotic (~2 min); (4) inflow of the pathogen via the fluidic port in the 3D-printed device is indicated by the blue arrow (~1 min); (5) incubation (~12 hr for *E. coli*); (6) readout of the resulting bacterial clearing and information on choosing antibiotics for the next test (~2 min). In steps 1 and 5, the heat bed of the 3D printer is used for fixing the print during printing (in step 1) and incubating the sample (in step 5). See [Supplemental Information](#) for a movie of the process.

device capable of both incubating pathogens and testing drug efficacy, thereby leading to an integrated system. The idea would be to have portable laboratory-like test facilities that could be more spread out than hospitals but still in locations where ease of access and repeat use would be possible. Using 3D printing in an approach such as this lends many advantages, such as the ability to produce inherently sterile structures (see below) with architectures that can be tailored to the individual application, with fluidic channels and internal voids as necessary. As well as being reconfigurable on demand to suit changing requirements, these structures are produced from cheap, biodegradable materials. Indeed, the emergence of 3D printing in health care is set to make a big impact.^{6–8} We propose a system that is fully automated and built by a combination of three elements: plastic printing, gel deposition, and drug spraying by an ink-jet array (Scheme 1).

RESULTS

Here, we present our efforts to design and build such a fully automated system. Our system is simple to use, and it is a fully portable independent diagnostic unit that can be used by untrained personnel in hospitals, in the offices of general practitioners, at home, or in the field. Bacterial samples can easily be introduced at one inlet via fluid injection and can be sampled in parallel over a number of lanes. The use of fused deposition modeling (FDM) printing has the advantage of producing intricate fluidics not easily accessible with injection molding, and the resulting devices are intrinsically sterile because of the deposition temperature of the print. In addition, it is easy to produce leak-free prints with the use of polylactic acid (PLA) in our configuration, and the devices can be autoclaved and reused as needed. PLA was chosen as a substrate for printing in our application because it is a cheap material with good properties for ease of 3D printing in that it produces water-tight structures with high fidelity to digital designs. Although other materials are available for FDM 3D

¹WestChem, School of Chemistry, University of Glasgow, Glasgow G12 8QQ, UK

²Lead Contact

*Correspondence: lee.cronin@glasgow.ac.uk
<http://dx.doi.org/10.1016/j.chempr.2016.08.008>

printing, we find PLA to be more than adequate for the application we describe. Our setup could, however, be used with other materials if required.

Normally, we needed only 0.2–0.3 mL of a 1 mL total bacterial sample volume. In this study, we used bioluminescent bacteria to explore and quantify the efficacy of three antibiotic drugs (kanamycin, tetracycline, and polymyxin B) against *Escherichia coli*. Bioluminescent bacteria allowed us to follow the experiment easily as proof of principle, but this is by no means necessary for the device to function (we show this to be the case here also). Although this is difficult to convey in a photograph, the growth zones of bacteria are clearly visible by eye, because the reflectivity of the agar surface changes significantly when bacteria grow on it (i.e., tilting the device in the light shows where bacteria have grown and where they have not). This approach can be used to identify bacteria that have not been transformed to be bioluminescent. We used clearing zones to assess the efficacy of the antibiotics. These model drugs effectively illustrate that the platform presented here can explore different types of antibiotic modes of operation (e.g., bacteriostatic and bactericidal). This system also builds upon our recent development of 3D-printed chemical “reactionware” for bespoke reagent and/or fluid control by using an easily accessible and configurable consumer 3D printer that can be customized mechanically with open-source software.^{9–11}

We have constructed a robotic platform based on a RepRap 3D printer¹² and expanded its capability to dispense gels and to handle very small amounts of liquid with the use of ink-jet technology (see [Figure 1](#)). The [Supplemental Information](#) provides the details for users to modify their own RepRap, and source codes (software and computer-aided designs) are freely available for non-profit use (STL files for the modified 3D printer parts are also available from the authors). The robot uses a conventional FDM 3D printer, in which a molten polymer is extruded through a 0.45 mm nozzle and deposited in a layer-by-layer fashion to create the 3D-printed test device. The operating principle of this type of 3D printing, in which polymers are heated to between 180°C and 350°C depending on the polymer to be printed,¹³ produces inherently sterile structures, an unexplored feature that is perfect for biological applications because sterile conditions are a must. We propose that the devices should be sealed to maintain sterility after manufacturing (like any sterile laboratory consumable), or the whole system can be sterilized and placed in a suitably sterile environment, such as a flow hood.

Traditionally, unknown bacterial pathogens are isolated and cultured to obtain an antibiogram.¹⁴ Antibiograms can be obtained via agar diffusion, agar dilution, Etest, and broth microdilution. The most common is a semi-quantitative agar diffusion test that places paper discs infused with a particular antibiotic onto a bacterial lawn, and then the effectiveness of the antibiotic is assessed by measurement of the clearing diameter around the discs. The main advantage of the disc test is the ability to assess several antibiotics in parallel; however, it is not fully quantitative. The Etest was developed to solve the semi-quantitative nature of disc tests. It is a simple system utilizing a testing strip impregnated with an increasing concentration of the subject antibiotic, allowing the minimal inhibitory concentration (MIC) of the antibiotic to be determined. Other test methodologies, such as broth microdilution and agar dilution, yield quantitative results by exposing liquid or plated cultures to a serial dilution of antibiotics. However, to get quantitative results, most of these systems are labor intensive and require specialized personnel.

Our approach combines the advantages of all methods described above by producing aligned diffusion tests in an automated setup, where individual antibiotics are

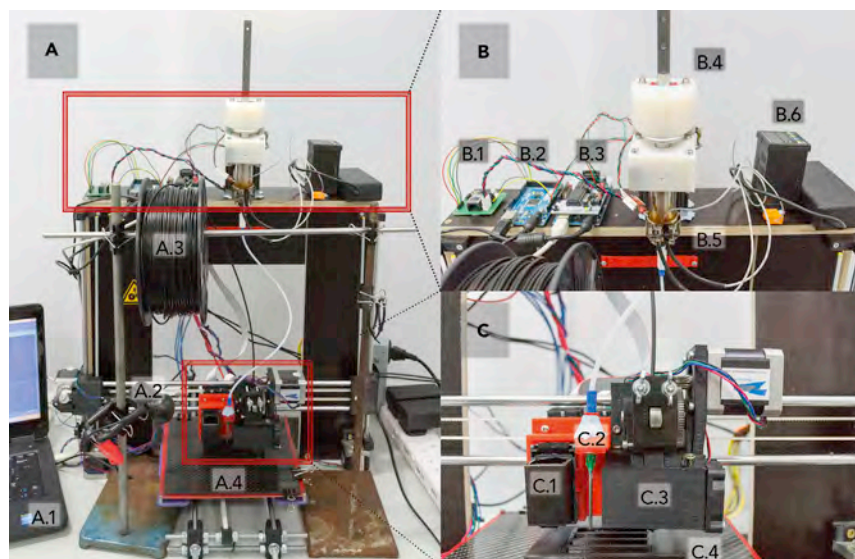


Figure 1. The 3D-Printer-Based Robotic Setup

(A) Image of the robotic setup: (A.1) computer, (A.2) webcam for monitoring, (A.3) PLA filament, and (A.4) printing bed.

(B) Close-up of the control electronics and the agar pump: (B.1) motor driver for the pump, (B.2) Arduino Mega 2560 Rev. 3 to control the pump, (B.3) ink shield on the Arduino Mega 2560 Rev. 3 to control the ink cartridge, (B.4) pump built in house to dispense agar, (B.5) heating mantle to keep the agar solution at 70°C, and (B.6) temperature controller for the heating mantle.

(C) Close-up of the carriage: (C.1) ink cartridge filled with antibiotic solution, (C.2) needle for dispensing the agar, (C.3) hot end for the FDM 3D printing process, and (C.4) the printed device.

deposited via ink-jet printing onto aligned lanes of agar rather than one large Petri dish. The amount of antibiotic deposited can be tuned by varying the spray time, eliminating the need to produce test solutions of different concentrations. The aligned nature of the diffusion test makes comparison between different concentrations of the same antibiotic possible by eye rather than requiring a measurement. The fact that any amount of antibiotic can be supplied as needed makes it feasible to determine the MIC of different antibiotics in an automated fashion. This allows decisions about treatments, potentially avoiding overuse of broad-spectrum antibiotics or validation of potential combination therapies on demand.

For the purposes of our study presented here, we designed a device with four chambers (1 cm × 5 cm; [Figure 2](#)), each connected with a channel to the same inlet port and filled by the robot with a growth medium, typically an agar gel. However, the number of chambers can easily be modified. Once the gel is deposited in the test chambers, the antibiotic is automatically sprayed into the chamber. Either different amounts of the same antibiotic or three different antibiotics plus a blank test are sprayed. Typically, preparing a device requires 4 hr, but this could be reduced significantly with simple optimizations, such as reduction of overall device size, more lanes per device (which would reduce the per-lane print time), fewer lanes per device (e.g., if only two antibiotics are to be compared), or a more sophisticated printer that can print at higher speeds if required ([Scheme 1](#)). In the final step, the device is covered with a 3D-printed lid. A full technical description of the robot and modes of operation, as well as the source code, 3D models, and order codes for all components, can be found in the [Supplemental Information](#) (see sections “Robot Design and Construction” and “Process Control Software,” [Figures S1–S4](#), and [Schemes S1–S3](#)). We found the printed devices to be robust with no

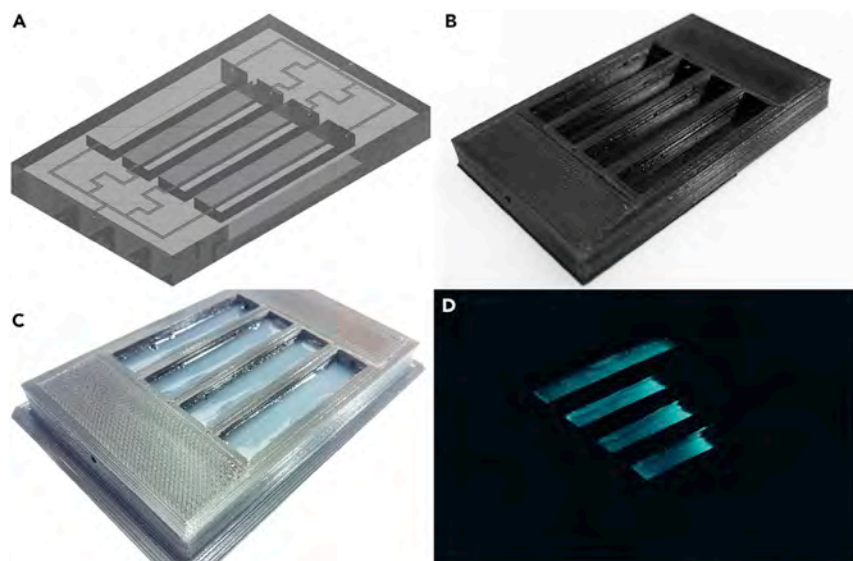


Figure 2. Stages of the Device from Design to Real Use

- (A) Visualization of the device design.
(B) The printed device.
(C) The device after the robot deposited the agar and the antibiotic.
(D) The device in the dark with bioluminescent bacteria.

evidence of leakage of either growth medium or bacterial culture in any of our experiments.

To demonstrate the applicability of these devices as performance tests for antibiotics, we selected *E. coli* DH5 α and investigated several methods for assessing antibiotic performance. As model systems, we tested three antibiotics: kanamycin, tetracycline, and polymyxin B. They were chosen because they represent three different modes of operation; kanamycin is an aminoglycoside bactericidal antibiotic,¹⁵ tetracycline is a broad-spectrum bacteriostatic antibiotic,¹⁶ and polymyxin B is a bactericidal amphiphile that destroys the cell membrane of gram-negative bacteria.^{17,18} These three antibiotics require different solvent compositions. Kanamycin is soluble in water, tetracycline is soluble in water/ethanol mixtures (here, we used a stock solution of 5 $\mu\text{g}/\mu\text{L}$ in 70% EtOH/H₂O, which was subsequently diluted with sterile water to produce the desired concentrations), and polymyxin B is a surfactant in water. To aid our test experiments by visualizing growth, we used *E. coli* that was engineered to become bioluminescent and resistant to ampicillin by transformation of pXen13 (PerkinElmer) plasmid (Figure 3; the full experimental procedure is provided in the Supplemental Information). This provides a test that can assess metabolic activity because only the living bacteria are bioluminescent. Here, we found that for the strain of *E. coli* used, the clearing per antibiotic followed the expected trend for diffusion in gels. Importantly, we were also able to easily see bacterial growth by eye without the need for bioluminescence, allowing us to further validate the potential of this approach for widespread use in the field (Figure 3). For general use of our system, it would be impractical to use only bacteria that had been transformed to be bioluminescent; therefore, visual identification of the extent of bacterial growth should be seen as the standard approach for this technique. The transformed bacteria were used only to confirm that the areas of bacterial growth identified visually were coincident with the areas of bacterial metabolic activity.

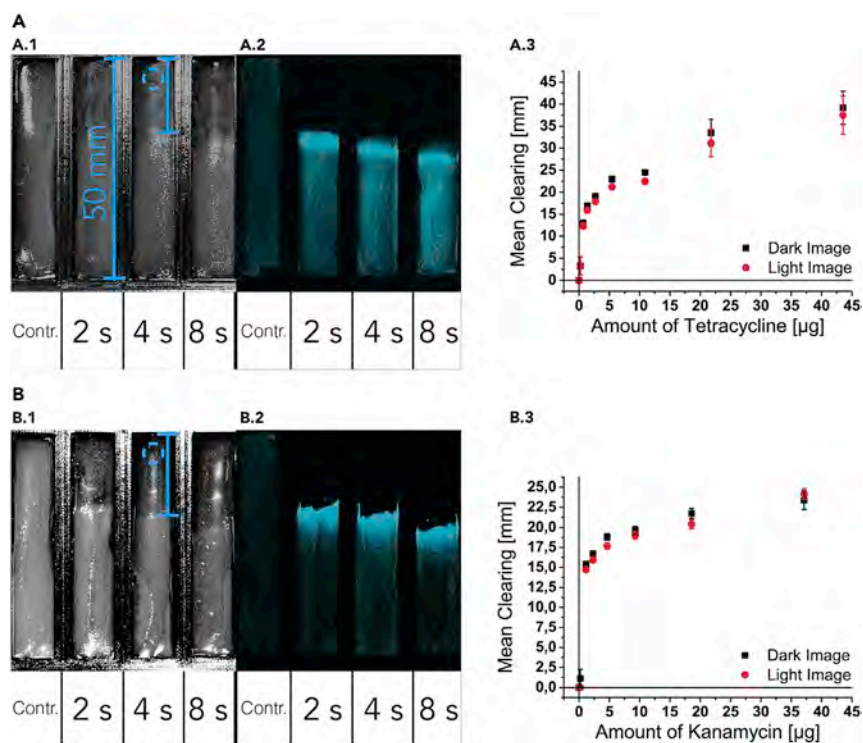


Figure 3. Inhibition Tests with Tetracycline

(A) Lanes from left to right: (A.1) ampicillin control (negative test) and 1/5 diluted tetracycline stock sprayed for 2 s (scale bar represents 50 mm), 4 s (scale bar represents the measured bacterial clearing due to antibiotic activity), and 8 s; (A.2) the same test plate as in (A.1) but photographed in the dark; (A.3) summary of clearing experiments measured in the light (red circles) and dark (black squares) with various amounts of tetracycline. The mean clearing was taken from at least six experiments, and error bars represent the SEM (see section “Tetracycline Experiments” in the [Supplemental Information](#) for the full procedure).

(B) Inhibition tests with kanamycin. Lanes from left to right: (B.1) ampicillin control (negative test) and 1/5 diluted kanamycin stock sprayed for 2 s, 4 s (scale bar represents the measured bacterial clearing due to antibiotic activity), and 8 s; (B.2) the same test plate as in (B.1) but photographed in the dark; (B.3) summary of the clearing experiments measured in the light (red circles) and dark (black squares) with various amounts of kanamycin. The mean clearing was taken from at least six experiments, and error bars represent the SEM (see section “Kanamycin Experiments” in the [Supplemental Information](#) for the full procedure). Images A.1 and B.1 were converted to grayscale and contrast enhanced so the bacterial lawn would be more visible in the photographs. When viewed by eye, the edge of the bacterial clearing was easily visible. For comparison, see the original full-sized photographs in [Figure S10](#). The spray point of the antibiotic is indicated for one lane in both light photographs (blue broken circle), and the clearing measurement is also indicated (blue bar). For the full procedure, see the [Supplemental Information](#).

We are able to deposit different amounts of antibiotic ranging from 0.02 to 43.5 μg on to the gel to assess bacterial susceptibility ([Figure 3](#)). For example, kanamycin cleared an average of 24.2 ± 0.68 mm at 37.1 μg deposition. Tetracycline cleared an average of 27.5 ± 3.4 mm at a deposition of 43.5 μg (\pm represents the SEM). The clearing profiles and reported variation in clearing matched the expected clearing measurements. However, we were unable to get consistent clearing of polymyxin B because of its surfactant nature ([Figure S22](#)). In addition, experiments to further assess different approaches for evaluating the performance of antibiotics were conducted. In each case, one of the four lanes of the device was used as a negative control, i.e., only ampicillin was added to the agar to prevent contamination. The other lanes were treated with the same amount (30 μg each) of different antibiotics for comparison of

their effectiveness (Figure S23). Two different antibiotics, kanamycin and tetracycline, showed different clearances of *E. coli* at the same nominal concentration.

Although this is not unexpected, given that the MICs of all three antibiotics are different, it illustrates nicely how comparing the clearing by eye becomes much easier in linear arrangements than in common circular clearings (Figure S25 illustrates this). This demonstrates not only that this approach offers the same capability as the classic agar diffusion test but also that the linear arrangement of the test lanes allows much quicker and easier readout of results. Moreover, it is trivial to add a pre-calibrated ruler to the 3D model of the dish to aid quantitative analysis of the clearing. To investigate reusability, we autoclaved the printed devices three times and found no considerable degradation (i.e., deformation to a degree that would make a ruler too inaccurate). In a second set of experiments, three lanes of the device were sprayed with different solution volumes of the same antibiotic concentration (wt %) or with the same solution volumes of different antibiotic concentrations. This was to establish the amount of antibiotic that the microorganism would be susceptible to (Figure 3). This approach provides a test to ensure that the mode of deposition does not influence the result of the experiment. A given amount of antibiotic was deposited three different ways: (1) spraying an antibiotic solution of low concentration for a long time (i.e., depositing 2.32 μg by spraying a 1 $\mu\text{g}/\mu\text{L}$ antibiotic solution for 4 s), (2) spraying an antibiotic solution of high concentration for a short time (i.e., depositing 2.32 μg by spraying a 2 $\mu\text{g}/\mu\text{L}$ antibiotic solution for 2 s), and (3) spraying an antibiotic solution of low concentration several times for short periods and drying the drop in between (e.g., depositing 18.56 μg of kanamycin [2 $\mu\text{g}/\mu\text{L}$] by spraying several times for a short amount of time [4 s] and letting the droplet dry for 2 min in between). The third deposition method ensures that the larger droplet created by spraying for a long time does not alter the result of the test (see Figure 4 and Supplemental Information section "Statistical Analysis of Different AB Deposition Modes"). None of the modes of deposition altered the clearing data we collected, and only the total amount of antibiotic deposited determined the clearing distance (see Supplemental Information section "Antibiotic Experiment Analysis"). To rigorously verify this, we performed various statistical analyses on sets of obtained data by spraying 1.16, 2.32, 4.64, 9.28, 18.56, and 37.12 μg of kanamycin. See section "Statistical Analysis of Different AB Deposition Modes" in the Supplemental Information for graphs and a more extensive description of the tests.

These tests yielded results well within the margin of error of commercially available antibiotic test discs (BD Sensi-Discs), which state a variability of 8 mm in clearing, providing all the advantages of quantitative testing. To determine the amount of antibiotic deposited, we created calibration curves for the respective solvent compositions by spraying pure solvent onto glass slides and weighing them after various spraying times. The deposition of pure solvent was found to be 579 and 654 $\mu\text{g}/\text{s}$ for water and 14% ethanol in water, respectively; in both cases, the deposition was linear with time (Figures S6 and S7). The increase in deposition for a mixed solvent is expected given the nature of the ink cartridge, which is designed to flash evaporate ink that has a volatile component.

Finally, as a proof of concept, we did an experiment where only a combination of different antibiotics would result in complete clearing of the pathogens. This allowed us to explore a case where a sample has multiple pathogens, which would be useful when a patient has multiple infections. Alternatively, we could also investigate the conditions under which only one type of bacteria needs to be eliminated while another given bacteria should be left unaffected. To do this experiment,

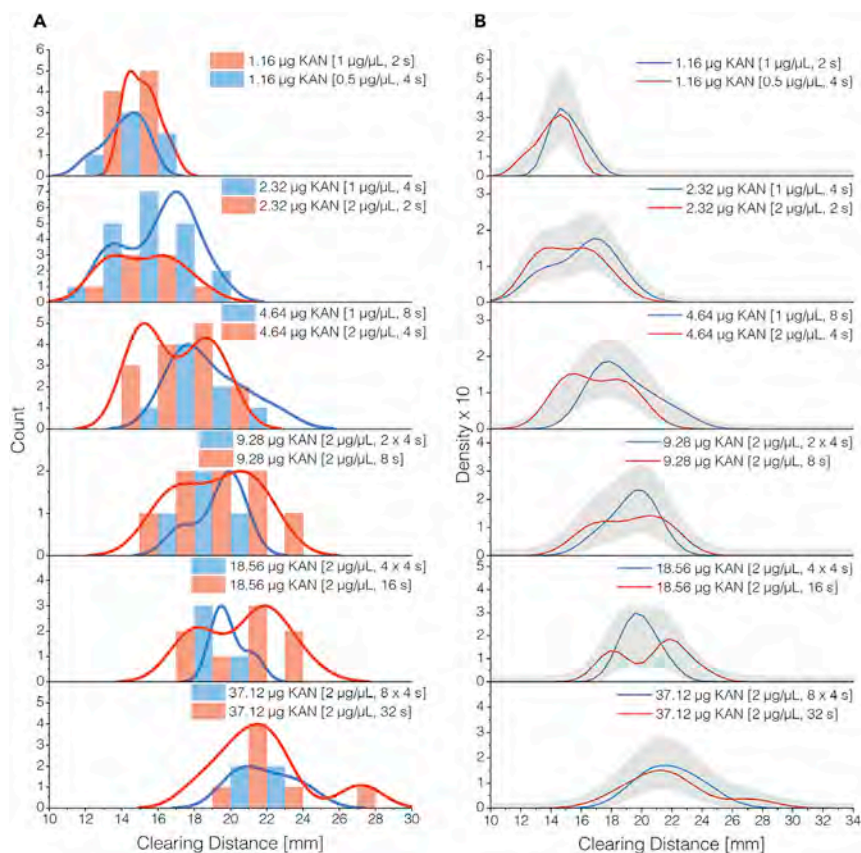


Figure 4. Comparison of the Clearing Data Obtained from Different Modes of Depositing the Same Amount of Kanamycin

(A) Histograms of the raw data are overlaid with kernel smooth plots generated with OriginPro 2015 SR1.

(B) Plots comparing kernel density include 95% confidence intervals (gray shaded areas) produced with `sm.density.compare` from the `sm` package in R (see section "Statistical Analysis of Different AB Deposition Modes" in the [Supplemental Information](#) for full details).

we did not add ampicillin to the growth medium, and the LB agar was replaced with BluO-gal and isopropyl β -D-1-thiogalactopyranoside (100 and 4 $\mu\text{g}/\text{mL}$, respectively; both from Life Technologies). The medium was deposited as in the previous experiments. We left the leftmost lane blank to see whether any contaminants would grow. Ampicillin (100 $\mu\text{g}/\text{mL}$) was sprayed for 16 s in the next lane, kanamycin (2 $\mu\text{g}/\text{mL}$) was sprayed for 16 s in the adjacent lane, and both ampicillin and kanamycin were sprayed for 16 s on top of each other in the final lane. A total volume of 60 μL of *E. coli* culture at a ratio of 6:1 (pXen13:pHSG299) was added into each lane, and the bacteria were allowed to grow overnight at 37°C. As a result, each of the two center lanes cleared only one of the two pathogens, and only the rightmost lane cleared both (see section "Antibiotic Formulation" in the [Supplemental Information](#) and [Figure S26](#)). As a final test, we compared the performance of the presented apparatus and methodology with that of commercial disc tests by spraying the same amount of antibiotic contained in a disc directly onto one of the lanes of the device ([Figure 5](#)).

Here, the antibiotic that was sprayed cleared slightly more (~15% for kanamycin and 14% for tetracycline, each at 30 μg ; [Figure S24](#)) than an antibiotic disc. This is explained by the fact that the solution of antibiotic diffuses directly into the agar when deposited and becomes fully effective, whereas an infused disc itself acts as

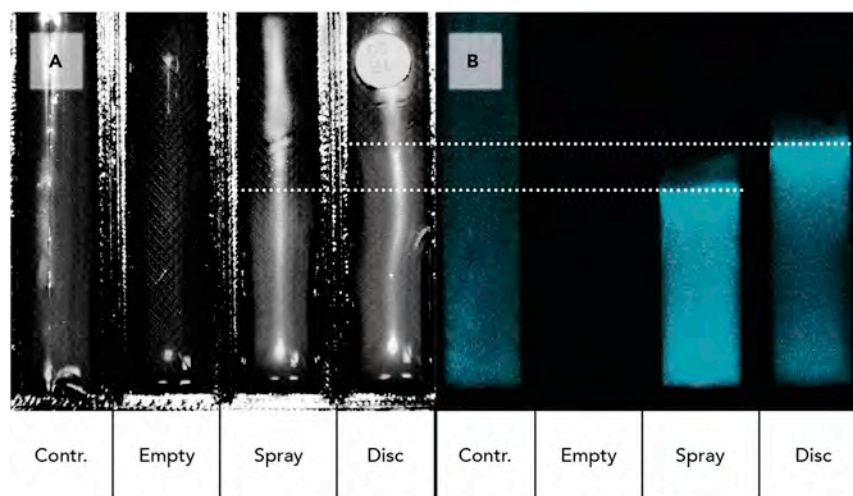


Figure 5. Comparison of a Commercially Available Antibiotic Disc Test with the Robotic Setup

From left to right, the first lane (contr.) constitutes the negative test, containing only ampicillin. The second lane (empty) was unused for this experiment. In the third spray lane, 30 μg of tetracycline was sprayed down. In the last disc lane, a paper disc infused with 30 μg of tetracycline was placed at the same height as the sprayed antibiotic. Lanes are shown both in the light (A) and in the dark (B). The image in (A) was converted to grayscale and contrast enhanced so the bacterial lawn would be more visible in the photographs. When viewed by eye, the edge of the bacterial clearing was easily visible. For comparison, see original full-sized photographs in [Figure S24](#).

a diffusion barrier, preventing it from releasing all of the antibiotic contained in the disc into the gel underneath. This illustrates not only that discs have their own drawback of being a physical object obstructing the observation of very small amounts of clearance (i.e., the minimal observable diameter is slightly larger than the physical diameter of the disc) but also that the concentration of antibiotic actually present in the agar is not precisely known. The use of defined agar lanes yields a better spatial resolution of the clearance because diffusion does not occur in a circular fashion; rather, the locally high concentration at the disc or spray point diffuses quasi-linearly down the lanes. This steeper gradient causes the antibiotics to diffuse further and hence results in better resolution of the clearing or a faster result because small clearings become visible earlier. For the BBL Sensi-Disc with 30 μg of kanamycin, the expected clearance stated by the manufacturer for *E. coli* (ATCC 25922) is 17–25 mm in diameter (i.e., 8.5–12.5 mm from the center of the disc; see section “Comparison with Commercial Disc Tests” in the [Supplemental Information](#)), whereas it cleared 20.7 mm in our lanes. The same was observed when we sprayed the antibiotic. On circular Petri dishes, the disc with the sprayed antibiotic cleared a circle of a 12.75 mm radius, and in the lanes, the clearing extended 23.55 mm from the center.

DISCUSSION

In conclusion, we have developed an autonomous robotic system that combines 3D printing, gel deposition, and ink-jet technologies into a unified platform. We used this system to determine and compare the antibacterial activity of three standard antibiotic agents with different mechanisms of action, similar to standard disc diffusion systems. The robotic platform was used to 3D print a bespoke test device, which was filled with growth medium via a syringe-based liquid handling system, and finally microgram quantities of the antibacterial agents were deposited by an ink-jet process. This system, which involves one automated, small-form-factor device that

does not need expert operation and can be used virtually anywhere at a very low cost (~\$0.10 per test),¹⁹ was found to replicate and surpass many aspects of the traditional techniques, especially in the ability to use one antibiotic solution “cartridge” to accurately deposit any desired quantity of material for testing. Furthermore, the use of PLA as a print material did not give any issues with leaking or absorption of water from the environment during our studies.²⁰

Beyond the experimental results presented here, we envisage that our system’s design could enable many further modes of operation to address a range of other possible applications. Although a single self-contained test might be useful in a research laboratory, in a hospital environment, the robot could be used to mass produce test devices that are placed onto the robot again when needed and are only then filled with fresh agar and antibiotic (see section “Process Control Software” in the [Supplemental Information](#) for a detailed explanation of the different modes of operation). The advantage of decoupling device printing from agar and antibiotic filling is that the actual test is sped up considerably. With pre-printed and autoclaved test devices, we easily achieved 128 single tests performed by one person in less than one working day (without incubation time; see [Figure S4](#) for an image of a stack of plates prepared in a few hours). Additionally, it would be reasonable to mimic the procedure of the standard reference agar dilution test by using the ink-jet to deposit a well-defined layer of antibiotic and then seeding several pathogens per lane. Moreover, the robot could assist the classic broth microdilution test because microgram amounts of antibiotics can be added on demand. Because of the precision of the ink-jet process, it would take just minutes to produce a full dilution series from a single cartridge of known concentration. Lastly, in addition to being able to cover many existing test methodologies in one single automated apparatus, the setup presented can be used to easily produce any mixed antibiotic formulation ([Figure S26](#)); which would be impossible with discs or Etests and would make the already labor-intensive broth microdilution or agar dilution more cumbersome. Mixing any number of antibiotics can then be achieved like dialing up a color on a standard ink-jet printer that mixes the different colors from the cartridges to give the required ink ratio.

We believe that researchers and clinicians can use this open hardware platform to quickly screen antibiotics or even assess entirely new formulations by any of the established techniques in a fully automated fashion. We envisage that this system can be extended to in-the-field discovery of the best antibiotic therapy to be used on a per infection basis. This system is another step in the use of integrated open technologies for exploring diagnostic hybrid biomaterial devices.²¹ In this case, we believe the system could become an important open-source²² approach in the fight against antibiotic-resistant microbes because the use of 3D printers and open-source software means that such configurable diagnostics could be deployed on a global scale for a fraction of the current cost.

EXPERIMENTAL PROCEDURES

Because the construction of the robotic platform and the programming thereof require a long and detailed technical description, please refer to the [Supplemental Information](#), which includes 3D models and source code for all programs.

SUPPLEMENTAL INFORMATION

Supplemental Information includes Supplemental Experimental Procedures, 27 figures, 15 tables, 3 schemes, and 1 movie and can be found with this article online at <http://dx.doi.org/10.1016/j.chempr.2016.08.008>.

AUTHOR CONTRIBUTIONS

L.C. conceived the original idea, and L.C., M.H., and S.G. adapted and designed the project. L.C. coordinated the efforts of the research team with help from S.G. S.G. built and programmed the robotic platform. S.S. helped build additional parts of the platform. M.H. transformed and cultured the bacteria. P.S.G. helped S.G. with the statistical analysis. M.H., P.K., S.S., and S.G. conducted and analyzed the experiments. P.K. generated the time-lapse video of the process. L.C. and S.G. co-wrote the manuscript with input from all co-authors. All authors co-wrote the [Supplemental Information](#).

ACKNOWLEDGMENTS

We gratefully acknowledge financial support from the EPSRC (grants EP/H024107/1, EP/I033459/1, and EP/J015156/1) and the Royal-Society Wolfson Foundation (a merit award). We are grateful to R. Exit for advice on system independence and A. MacDonnell for help with the artwork.

Received: April 11, 2016

Revised: August 5, 2016

Accepted: August 18, 2016

Published: September 8, 2016

REFERENCES AND NOTES

1. Boucher, H.W., Talbot, G.H., Bradley, J.S., Edwards, J.E., Gilbert, D., Rice, L.B., Scheld, M., Spellberg, B., and Bartlett, J. (2009). Bad bugs, no drugs: no ESKAPE! an update from the Infectious Diseases Society of America. *Clin. Infect. Dis.* **48**, 1–12.
2. World Health Organization. (2014). *Antimicrobial Resistance: Global Report on Surveillance* (WHO).
3. Deiss, F., Funes-Huacca, M.E., Bal, J., Tjhunga, K.F., and Derda, R. (2014). Antimicrobial susceptibility assays in paper-based portable culture devices. *Lab Chip* **14**, 167–171.
4. Weibull, E., Antypas, H., Kjäll, P., Brauner, A., Andersson-Svahn, H., and Richter-Dahlfors, A. (2014). Bacterial nanoscale cultures for phenotypic multiplexed antibiotic susceptibility testing. *J. Clin. Microbiol.* **52**, 3310–3317.
5. Lipson, H., and Kurman, M. (2013). *Fabricated: The New World of 3D Printing* (Wiley).
6. Johnson, B.N., Lancaster, K.Z., Hogue, I.B., Meng, F., Kong, Y.L., Enquist, L.W., and McAlpine, M.C. (2016). 3D printed nervous system on a chip. *Lab Chip* **16**, 1393–1400.
7. Mannoor, M.S., Jiang, Z., James, T., Kong, Y.L., Malatesta, K.A., Soboyejo, W.O., Verma, N., Gracias, D.H., and McAlpine, M.C. (2013). 3D printed bionic ears. *Nano Lett.* **13**, 2634–2639.
8. Gupta, M.K., Meng, F., Johnson, B.N., Kong, Y.L., Tian, L., Yeh, Y.-W., Masters, N., Singamaneni, S., and McAlpine, M.C. (2015). 3D printed programmable release capsules. *Nano Lett.* **15**, 5321–5329.
9. Kitson, P.J., Marshall, R.J., Long, D., Forgan, R.S., and Cronin, L. (2014). 3D printed high-throughput hydrothermal reactionware for discovery, optimization, and scale-up. *Angew. Chem. Int. Ed.* **53**, 12723–12728.
10. Kitson, P.J., Rosnes, M.H., Sans, V., Dragone, V., and Cronin, L. (2012). Configurable 3D-Printed millifluidic and microfluidic 'lab on a chip' reactionware devices. *Lab Chip* **12**, 3267–3271.
11. Kitson, P.J., Symes, M.D., Dragone, V., and Cronin, L. (2013). Combining 3D printing and liquid handling to produce user-friendly reactionware for chemical synthesis and purification. *Chem. Sci.* **4**, 3099–3103.
12. Jones, R., Haufe, P., Sells, E., Iravani, P., Olliver, V., Palmer, C., and Bowyer, A. (2011). Reprap - the replicating rapid prototyper. *Robotica* **29**, 177–191.
13. Gibson, I., Rosen, D., and Stucker, B. (2015). *Additive Manufacturing Technologies, Second Edition* (Springer-Verlag).
14. Cook, P.P., Catrou, P.G., Christie, J.D., Young, P.D., and Polk, R.E. (2004). Reduction in broad-spectrum antimicrobial use associated with no improvement in hospital antibiogram. *J. Antimicrob. Chemother.* **53**, 853–859.
15. Misumi, M., and Tanaka, N. (1980). Mechanism of inhibition of translocation by kanamycin and viomycin: a comparative study with fusidic acid. *Biochem. Biophys. Res. Commun.* **92**, 647–654.
16. Speer, B.S., Shoemaker, N.B., and Salyers, A.A. (1992). Bacterial resistance to tetracycline: mechanisms, transfer, and clinical significance. *Clin. Microbiol. Rev.* **5**, 387–399.
17. Wiese, A., Munstermann, M., Gutschmann, T., Lindner, B., Kawahara, K., Zahringer, U., and Seydel, U. (1998). Molecular mechanisms of polymyxin B-membrane interactions: direct correlation between surface charge density and self-promoted transport. *J. Membr. Biol.* **162**, 127–138.
18. Zavascki, A.P., Goldani, L.Z., Li, J., and Nation, R.L. (2007). Polymyxin B for the treatment of multidrug-resistant pathogens: a critical review. *J. Antimicrob. Chemother.* **60**, 1206–1215.
19. The cost of our 3D printer system is ~\$500, and the material cost per device is \$0.64. Allowing for at least ten uses per device and a system lifetime of at least 5 years would give a cost per test below \$0.10. This is for the current time and material needed for producing a device, although we believe this could be cut by a factor of at least 4. This would drop the cost to ca. \$0.025.
20. Kitson, P.J., Glatzel, S., Chen, W., Lin, C.-G., Song, Y.-F., and Cronin, L. (2016). 3D printing of versatile reactionware for chemical synthesis. *Nat. Protoc.* **11**, 920–936.
21. Paulsen, S.J., and Miller, J.S. (2015). Tissue vascularization through 3D printing: will technology bring us flow? *Dev. Dyn.* **244**, 629–640.
22. Trachtenberg, J.E., Mountziaris, P.M., Miller, J.S., Wettergreen, M., Kasper, F.K., and Mikos, A.G. (2014). Open-source three-dimensional printing of biodegradable polymer scaffolds for tissue engineering. *J. Biomed. Mater. Res. A* **102**, 4326–4335.